Hindawi
Advances in Mathematical Physics
Volume 2022, Article ID 3031117, 18 pages
https://doi.org/10.1155/2022/3031117

Research Article

Dynamical Analysis of Nonlocalized Wave Solutions of $(2+1)$-Dimensional CBS and RLW Equation with the Impact of Fractionality and Free Parameters

Nur Hasan Mahmud Shahen[1,2] **Foyjonnesa**[2] **Md. Rafiqul Islam**[3] **Ahmet Bekir**[4] **and M.M. Rahman**[2]

[1]*Department of Arts and Sciences, Bangladesh Army University of Science and Technology, Saidpur 5310, Bangladesh*
[2]*Department of Mathematics, Bangladesh University of Engineering and Technology, Dhaka 1000, Bangladesh*
[3]*Department of Mathematics, Bangabandhu Sheikh Mujibur Rahman Science and Technology University, Gopalgonj 8100, Bangladesh*
[4]*Neighborhood of Akcaglan, Imarli Street, Number: 28/4, 26030, Eskisehir, Turkey*

Correspondence should be addressed to M.M. Rahman; m71ramath@gmail.com

Received 22 April 2022; Revised 27 July 2022; Accepted 11 August 2022; Published 9 September 2022

Academic Editor: Mohammad Mirzazadeh

This study retrieves some new exact solutions to the $(2+1)$-dimensional Calogero-Bogoyavlenskii-Schilf (CSB) equation and regularized long wave (RLW) equation in the context of nonlinear traveling wave phenomena. In this regard, the advanced exp $(-\varphi(\xi))$-expansion method is imposed to the $(2+1)$-dimensional CBS and RLW equation, and consequently, rogue, kink, singular kink, periodic, singular, and multiple soliton solutions are exhibited in terms of trigonometric, hyperbolic, and rational function solutions. To enucleate the underlying nonlocalized traveling wave features, accomplished exact solutions are established by making their dynamic behavior of the exact solutions exhibited in three-dimensional (3D) and two-dimensional (2D) combined chart with the help of computational software Maple 18. All of our accomplished solutions are claimed to be new in the sense of conformable derivative, chosen a unique fractional type wave transformation, dynamical behavior of fractionally and free variable, and the imposed method on our preferred equations.

1. Introduction

Most of the physical problems are now formatted into mathematical schemes through partial differential equations (PDEs). In recent years, calculus of fractional nonlinear differential condition is one of the rising concern of nonlinear dynamics as well as plays an eventual role in real-life problems such as plasma physics [1], quantum mechanics [2], fluid mechanics [3], optical fibers [4], and other fields of applied mathematics and engineering. Calculus of fractional derivative is the generality of the traditional order of integration and differentiation and a conventional technique for demonstrating complex physical behavior, especially of the nonlinear mathematical science of engineering and physics. In the recent past, nonlinear fractional partial differential equations (FPDEs) have been inventing a potential platform for the researchers to interpret the tangible phenomena. As a result, some significant, concise, and original methods have been explored and explain to exact closed solutions of nonlinear FPDEs, videlicet, namely, the Hirota bilinear method [5, 6], modified extended tanh-function method [7], (G'/G)-expansion method [8], fractional subequation method [9], modified trial equation method [10], advanced exp $(-\varphi(\xi))$ method [11], tan $(-\varphi(\xi))$-expansion method [12], and improved Kudryashov method [13]. Recently, some researchers, like, Ferdous et al. [14], attained exact wave solutions to the extended Zakharov–Kuzetsov equation by implementing the generalized exp $(-\varphi(\xi))$-expansion

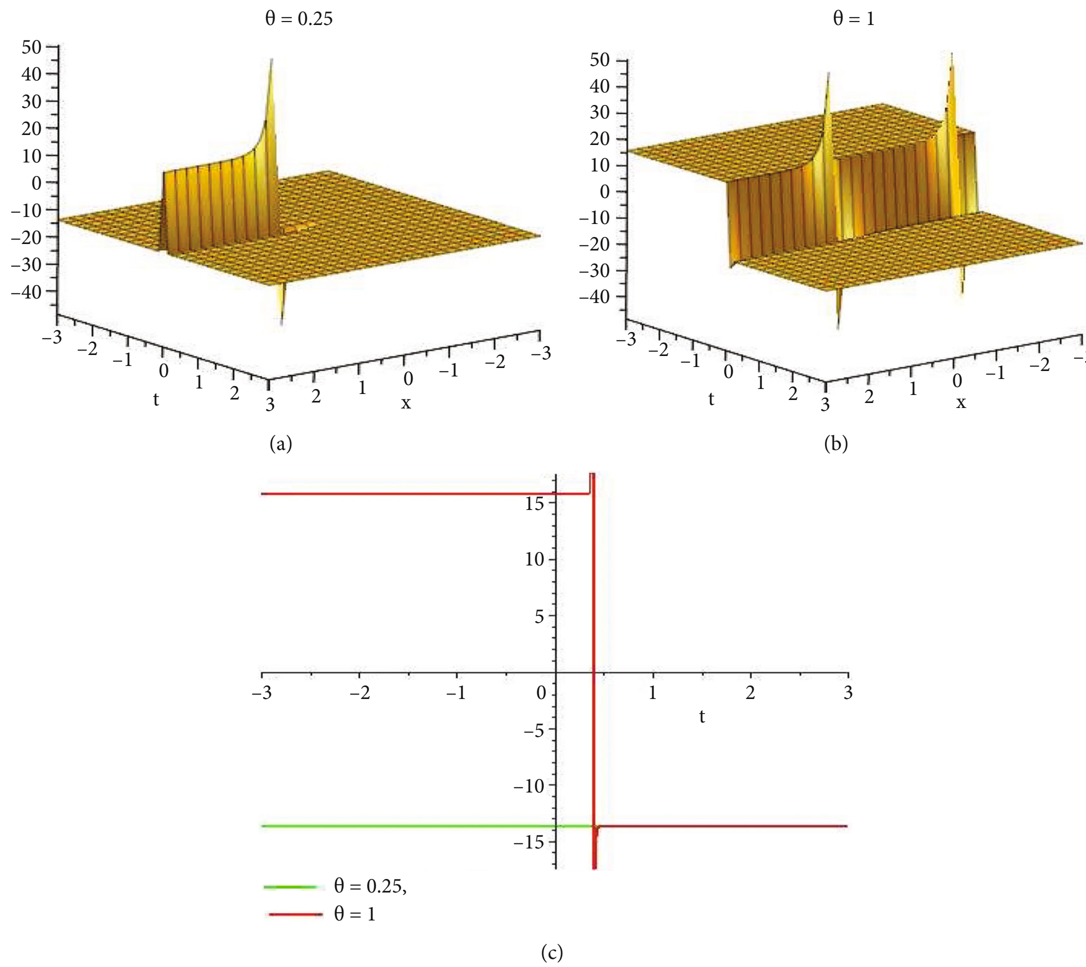

Figure 1: Dynamical behavior of function solution of $u_1(x, y, t)$. (a, b) 3D plot and (c) 2D combined plot for $x = 1$.

method. Alike, adopting the exp $(-\varphi(\xi))$-expansion modified technique, Khater [15] has established three different types of nonlocalized traveling wave solutions to the generalized Hirota-Satsuma (HS) couple KdV system. Encouraged by ongoing research on related topics, we extract the recent and more common precise solitary wave solutions to some nonlinear FPDEs, described earlier by proposing the advanced method of exp $(-\varphi(\xi))$-expansion, which can be considered the generalization of the generalized form of exp $(-\varphi(\xi))$-expansion [16].

Our current study mainly explores the dynamical changes of conformable time-fractional $(2+1)$-dimensional CSB equation [17] and regularized long wave (RLW) equation by employing the new progressive exp $(-\varphi(\xi))$ -expansion technique. Recent past, Rahman et al. [18] imposed this technique on some nonfractional NLEEs, but they did not show any productive concept to conformable nonlinear time fractional sense of NPEEs. We decisively believe that our stated advanced exp $(-\varphi(\xi))$ modified method will be frolicked a significant role in investigating the traveling wave arrangements of nonlinear science and mathematical physics. Here it is significant to note that our stated fractional equations are in a conformable sense so we have converted our equations in fractional form.

Consider the following generalized $(2 \quad +1)$-dimensional CBS conditions [19–22].

$$u_t + \phi(u)u_y = 0,\ \phi(u) = \partial_x{}^2 + au + bu_x\partial_x{}^{-1}, \tag{1}$$

or equivalently

$$u_t + u_{xxy} + auu_y + bv_x\partial_x{}^{-1}v_y = 0, \tag{2}$$

where $\partial_x{}^{-1} = \int f dx$ and a and b are two parameters. If we put dimensional exchange, $\partial_x = \partial_y$, then Equation (2) changes into a standard (KdV) equation. From there, Equation (2) can be written in the potential time fractional formation of $(2+1)$-dimensional CBS equation [17] with a conformable sense.

$$u_x N_t^\theta u + 4u_x u_{xy} + 2u_{xx}u_y + u_{xxy} = 0, t > 0, x, \quad y \in R, \tag{3}$$

where the coefficient of u and its higher derivative term is called the free variable and θ is a time derivative fractional-order parameter with an interval $0 < \theta \leq 1$.

Bogoyavlenskii and Schilf firstly originate this CBS equation in numerous ways [23]. For full possible indispensable

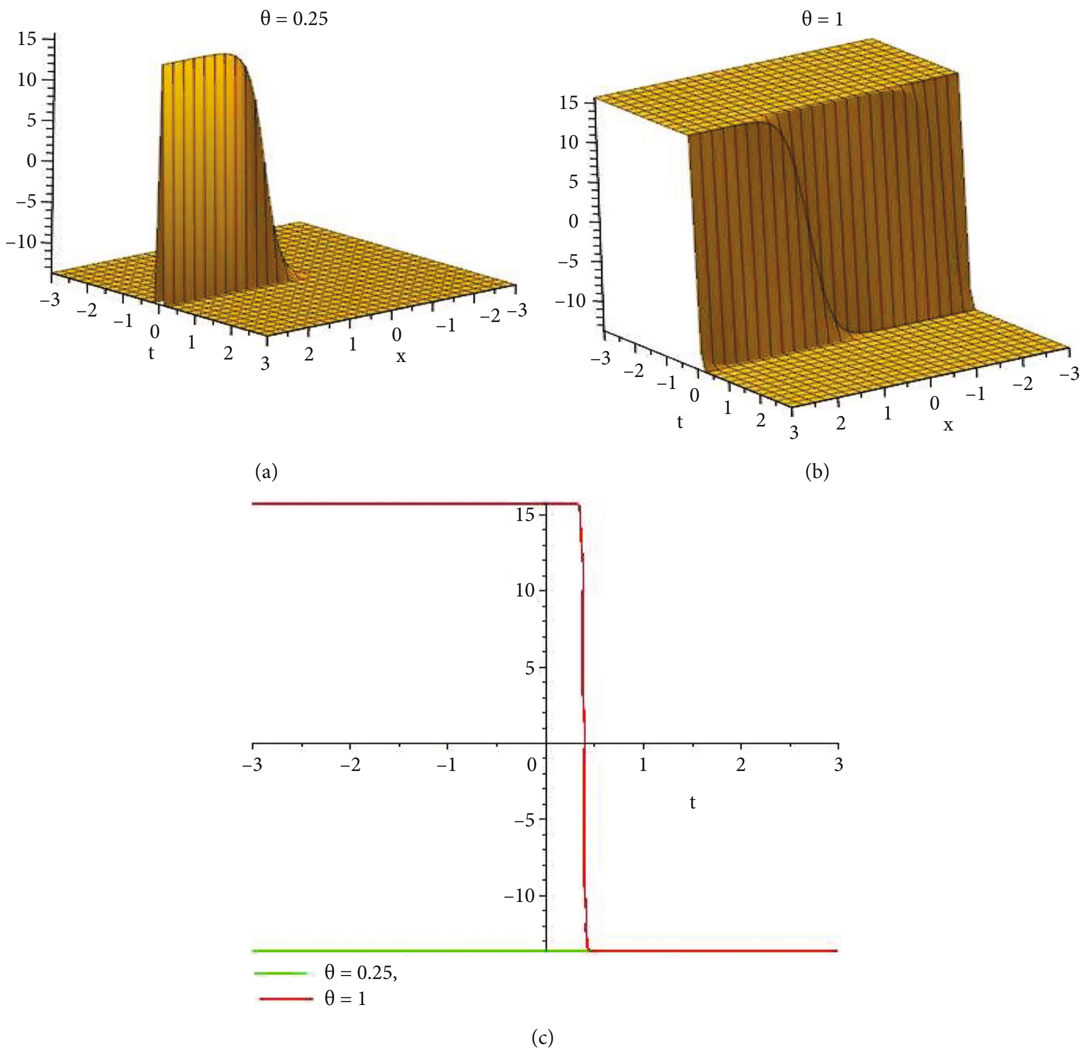

FIGURE 2: Dynamical behavior of function solution of $u_2(x, y, t)$. (a, b) 3D plot and (c) 2D combined plot for $x = 1$.

conditions, three effective procedures, to be specific the Backlund change strategy, the reverse Scaterin Scheme, and Hirota's bilinear approach [24–26], were minutely connected to get the precise arrangements of these equations. The CBS equation is resolved in numerous aspects of water wave mechanics, ocean science, nonlinear science, engineering mathematics, etc., under specific authoritative techniques such as the modified simple equation scheme, the Sin-Gordan expansion technique, the unified method, and the (G'/G)-expansion technique. [27–30]. To the best of our knowledge, our proposed advanced- exp $(-\varphi(\xi))$ expansion technique is not utilized yet to find the exact solutions of CBS equation with the concept of conformable derivative. Now we consider the time fractional regularized long wave (RLW) equation [31].

$$N_t^\theta u + u_x + \alpha(u^2)_x - u_{xx} N_t^\theta u = 0, \quad t > 0, \alpha, \quad \beta \in R, \quad (4)$$

where $0 < \theta \le 1$.

The RLW equation is a particular class of nonlinear conformable fractional equations that generates fruitful models for predicting the water wave and physical phenomena [32]. Many authoritative approaches have been the subject of investigating the RLW equation, such as the Fourier leap-frog method [33], finite difference method [34], Hirota direct method approach [35], and modified extended tanh method [36]. Whereas so far we know, with the sense of conformable derivative, there is no prolific results have not yet been established about our declared technique to simplify the RLW equation. The exact wave solutions of RLW equation we attained are completely new in respect of our mentioned method.

Recently, Ferdous et al. [14] proposed a generalized exp $(-\varphi(\xi))$-expansion method by choosing the auxiliary ODE of the form $\varphi'(\xi) - \lambda \exp(\varphi(\xi)) - \mu \exp(-\varphi(\xi)) = r$. In our mentioned method, we take the auxiliary nonlinear ODE of the form $\varphi'(\xi) - \lambda \exp(\varphi(\xi)) - \mu \exp(-\varphi(\xi)) = 0$ by setting $r = 0$. Here λ and μ are real type parameters, and reasonably, our said supplementary form affords much

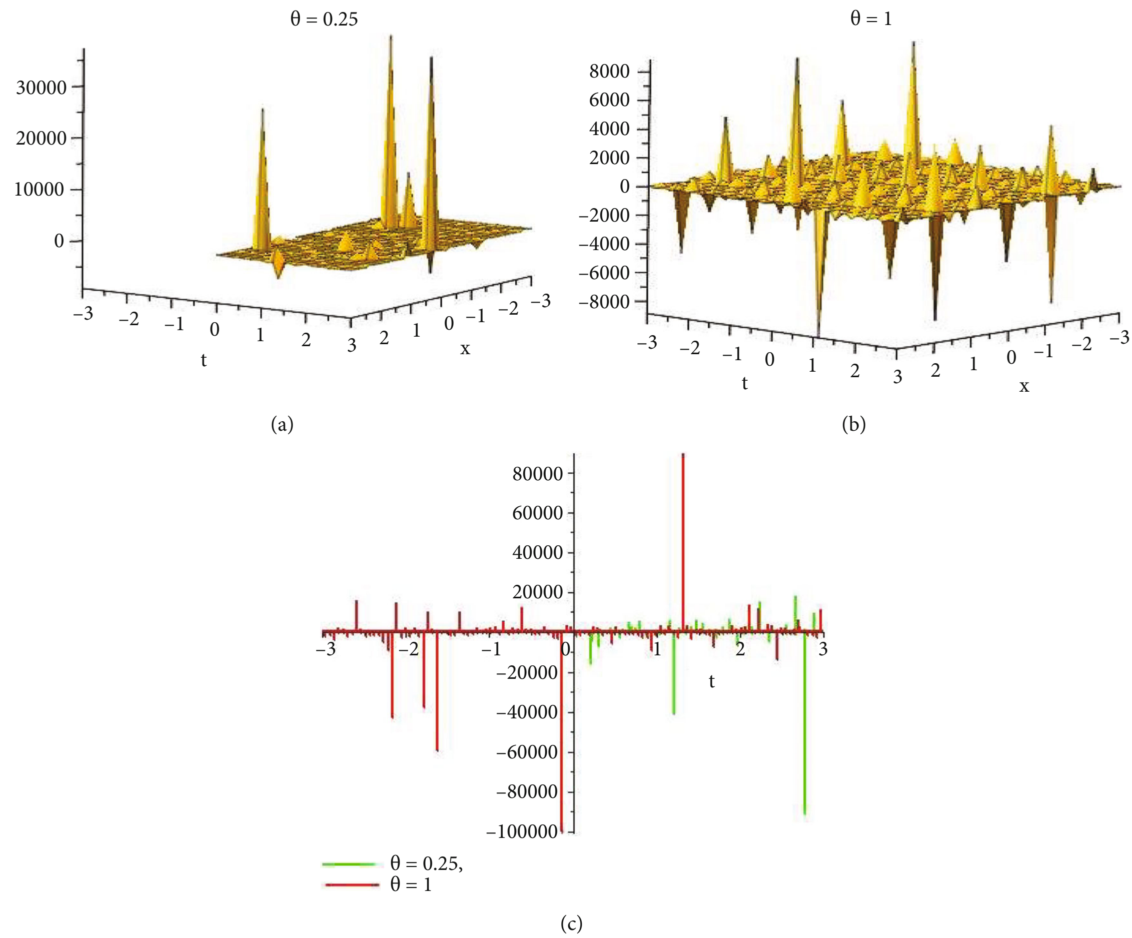

Figure 3: Dynamical behavior of function solution of $u_3(x, y, t)$. (a, b) 3D plot and (c) 2D combined plot for $x = 1$.

better complete solutions to the FPDEs as well as has a more comprehensive operational physical explanation than the findings of Ferdous et al. [14]. The important favor of our specified technique over the other approaches [15, 18] is that it provides some straight and succinct form of new exact wave solution, as well as it is very useful, well-organized, and responsive applicable in presenting of exact and explicit wave solutions to NPDEs, arises in science, mathematical physics, and engineering.

We have employed successfully the exp $(-\varphi(\xi)$ method on CBS and RLW equations to treasure the meticulous traveling wave solutions which have not appeared beforehand in publications.

We believe that our discoveries might be used to computer simulations of water waves in shallow water, to the study of the propagation of small amplitude long waves on the surface of shallow water, and to the advancement of scientific knowledge. Theoretical physicists, applied mathematicians, and ocean engineers who are interested in the precise solutions to moving rogue waves should all find this paper to be of interest. When this project is successfully completed, it may be possible to forecast the sea level of a coastal area during natural catastrophes. Low pressure systems like cyclones are the main culprits in natural disasters.

The paper's structure is as follows: the conformable derivative's narration and its elementary possessions are given in Section 2. The advanced exp $(-\varphi(\xi))$ expansion scheme has been outlined in Section 3. In Section 4, we apply this approach to the time-fractional $(2+1)$-dimensional equation of CBS and RLW. The findings and the debate are discussed in Section 5, and the conclusions are provided in Section 6.

2. Inceptions and Procedures

2.1. Definition and Some Features of Conformable Fractional Derivative. Khalil et al. [37] primarily exposed the sense of conformable derivative with a limit operator.

Definition 1. If $f : (0,\propto) \longrightarrow \Re$, then the conformable derivative with the fractional sense of f order δ is defined as

$$T_t^{\delta} f(t) = \lim_{\varepsilon \longrightarrow 0} \left(\frac{f\left(t + \varepsilon t^{1-\delta}\right) - f(t)}{\varepsilon} \right) \text{ for all } t > 0, 0 < \delta \leq 1. \tag{5}$$

Later, in the fractional-order method, Abdeljawad [38]

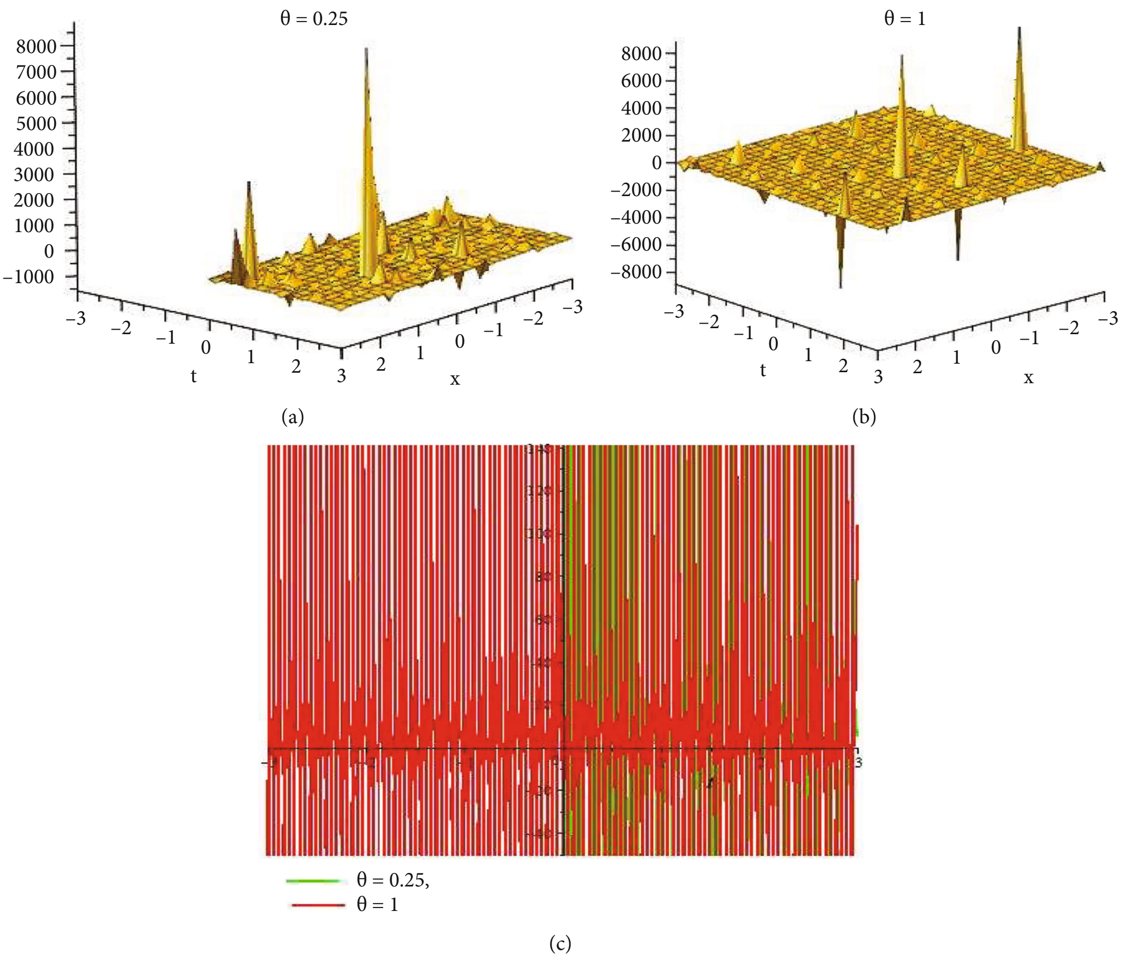

FIGURE 4: Dynamical behavior of function solution of $u_4(x, y, t)$. (a, b) 3D plot and (c) 2D combined plot for $x = 1$.

also discussed chain law, Gronwall's inequality, exponential functions, definite and infinite component integration, Taylor power series expansions, and Laplace transform conformable derivative. The difficulty of exiting the modified Riemann-Liouville derivative description [39] will efficiently resolve the concept of a conformable fractional-order derivative.

Theorem 2.

Let $\omega \in (0, 1]$ and $f = f(t)$, $g = g(t)$ be ω-conformably differentiable at a point $t > 0$; then,

(i) $T_t^{\omega}(cf + dg) = cT_t^{\omega} f + dT_t^{\omega} g$, *for all* $c, d \in \Re$

(ii) $T_t^{\omega}(t\gamma) = \gamma\, t^{\gamma-\omega}$, *for all* $\gamma \in \Re$

(iii) $T_t^{\omega}(fg) = gT_t^{\omega}(f) + f\, T_t^{\omega}(g)$,

(iv) $T_t^{\omega}(f/g) = gT_t^{\omega}(f) - f\, T_t^{\omega}(g)/g^2$

Moreover, if the function f is differentiable, then $T_t^{\omega}(f(t)) = t^{1-\omega} df/dt$.

Theorem 3. *Consider $f : (0, \omega) \longrightarrow R$ be a real type function such that f is differentiable and ω-conformable derivable. Also, assume that g be a derivable function well-defined in the range of f. Then, we have* $T_t^{\omega}(fog)(t) = t^{1-\omega} g(t)^{\omega-1} g'(t) T_t^{\omega}(f(t))_{t=g(t)}$, *where prime indicates the simple derivatives with respect to the point t.*

In this research, we have careful about the preferred equation with the concept of conformable-based derivative. In circumstance of basic calculus, numerous functions do not expand Taylor's power-order illustrations on specific points but in the technique of conformable-order derivative, they do consume the existence. CD accomplishes good in the product and chain rule while complicated plans appear in logic of basic fractional geometry. The CD of a constant type function is correspondent to zero wherever it is not the topic for Riemann derivative of fractional order. Mittag Leffler functions show a noteworthy authoritative in fractional-order calculus as interpretation to exponential function where the fractional-order form of exponential type function of the form $f(t) = e(t^{\alpha}/\alpha)$ seems in circumstance of CD.

3. Overview of the Method

In this division, we have considered our proposed advanced exp $(-\varphi(\xi))$-expansion scheme stepwise in brief. Assume a nonlinear time-fractional NPD equation in subsequent

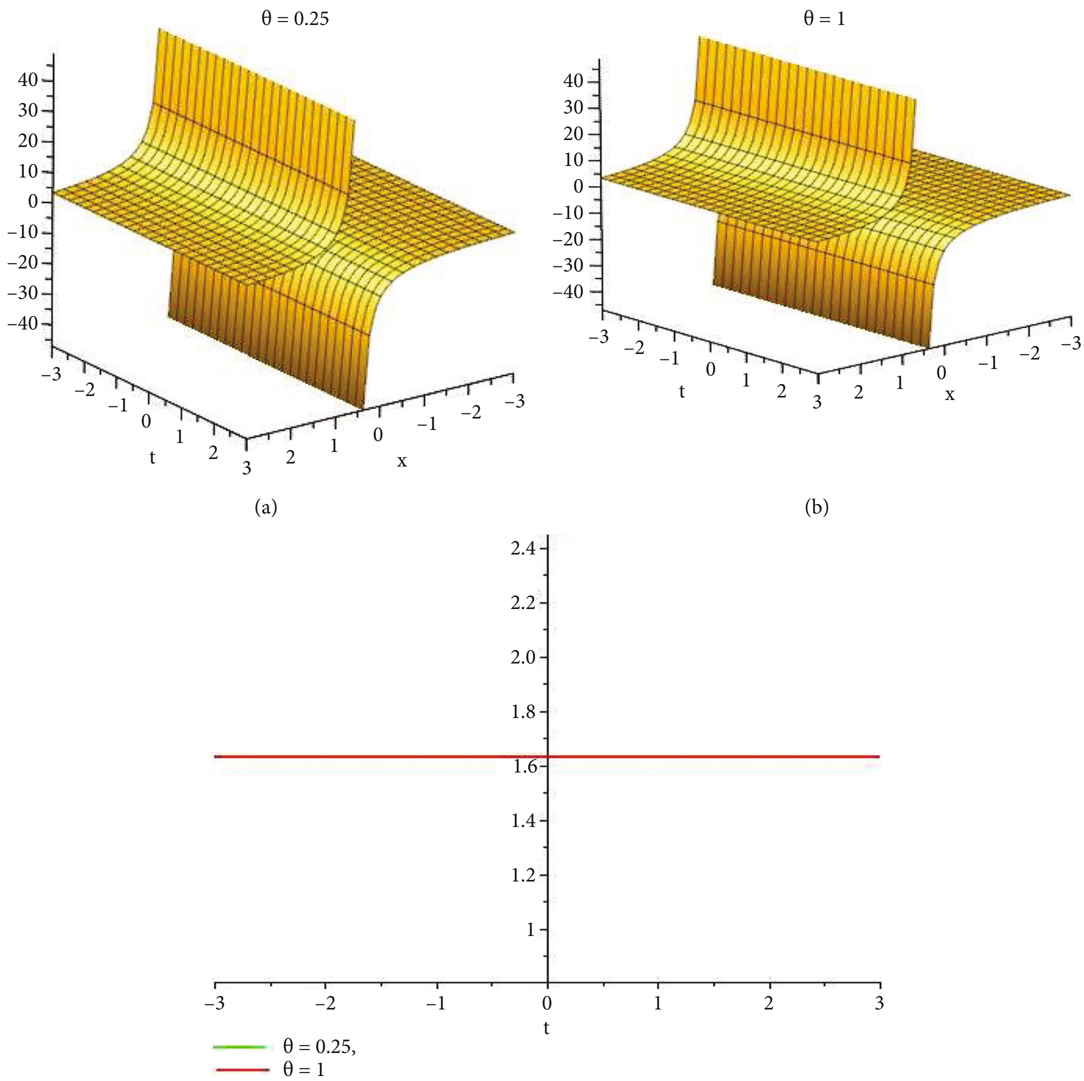

(a) (b) (c)

FIGURE 5: Dynamical behavior of function solution of $u_5(x, y, t)$. (a, b) 3D plot and (c) 2D combined plot for $x = 1$.

form,

$$\mathfrak{R}\left(\Pi, \Pi_x, T_t^{\theta}\Pi, \Pi_{xx}, T_{tt}^{2\theta}\Pi, \Pi_{xxx}, \cdots\cdots\right) = 0, \quad (6)$$

where $\Pi = \Pi(x, t)$ is defined as an unknown type function and $\mathfrak{R}$ denotes the polynomial of Π. It is a diverse type of PD, in through the nonlinear segment and the uppermost order of differential are involved.

Step 1. We deliberate a traveling variable for transferring the mentioned equation to nondimensionality. We alter all self-governing variable into a single variable, by the following way.

$$\Pi(x, t) = u(\xi), \xi = k\frac{x^{\eta}}{\eta} \pm V\frac{t^{\theta}}{\theta}. \quad (7)$$

By employing mentioned variable, Equation (7) allows us in dropping Equation (6) in ODE for $\Pi(x, t) = u(\xi)$ in the type

$$P\left(\cdots, u''', u'', u', u,\right) = 0. \quad (8)$$

Step 2. Let us consider that a polynomial can begin the solution of OD Equation (8) in the

$$\exp\left(-\varphi(\xi)\right) \text{ as } u = \sum_{i=0}^{N} A_i \exp\left(-\varphi(\xi)\right)^i, \quad A_N \neq 0. \quad (9)$$

Here N is the positive integer, which can be integrated by consistency of the highest order of derivatives to the highest order of nonlinear portions, performed in Equation (8).

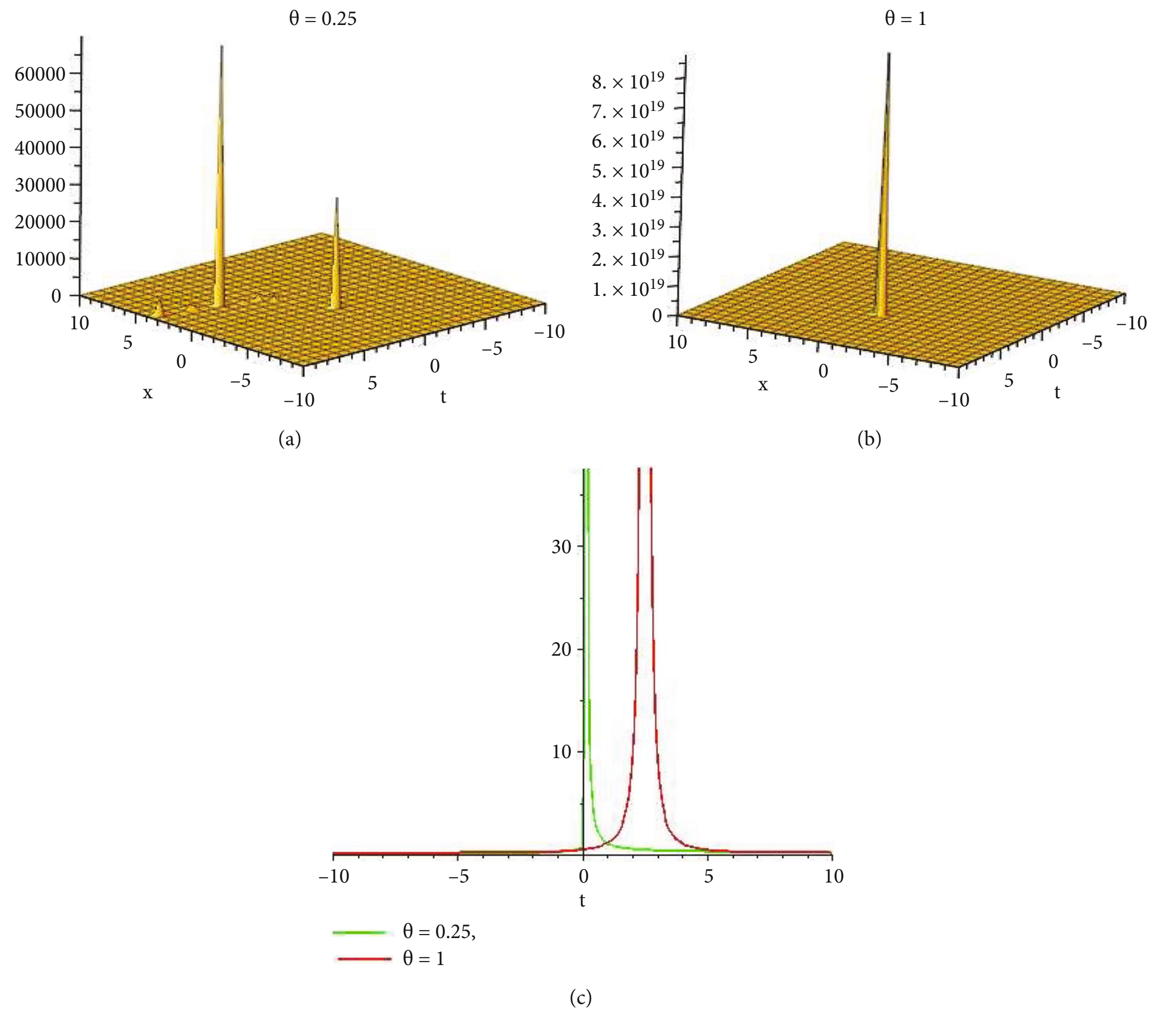

FIGURE 6: Dynamical behavior of function solution of $u_{6,7}(x,t)$. (a, b) 3D plot and (c) 2D combined plot for $x = 1$.

Also, the differential of $\varphi(\xi)$ satisfies ODE in the subsequent form

$$\varphi'(\xi) - \mu \exp\left(-\varphi(\xi)\right) - \lambda \exp\left(\varphi(\xi)\right) = 0, \tag{10}$$

and then, the function solutions of ODE Equation (8) are of the form.

Case 1. The function solutions are hyperbolic (when $\lambda\mu < 0$):

$$\begin{aligned} \varphi(\xi) &= \ln\left(\sqrt{\frac{\lambda}{-\mu}}\tanh\left(\sqrt{-\lambda\mu}(\xi + C)\right)\right), \\ \varphi(\xi) &= \ln\left(\sqrt{\frac{\lambda}{-\mu}}\coth\left(\sqrt{-\lambda\mu}(\xi + C)\right)\right). \end{aligned} \tag{11}$$

Case 2. The function solutions are trigonometric (when $\lambda\mu > 0$):

$$\begin{aligned} \varphi(\xi) &= \ln\left(\sqrt{\frac{\lambda}{\mu}}\tan\left(\sqrt{\lambda\mu}(\xi + C)\right)\right), \\ \varphi(\xi) &= \ln\left(-\sqrt{\frac{\lambda}{\mu}}\cot\left(\sqrt{\lambda\mu}(\xi + C)\right)\right). \end{aligned} \tag{12}$$

Case 3. When $\mu > 0$ and $\lambda = 0$,

$$\varphi(\xi) = \ln\left(\frac{1}{-\mu(\xi + C)}\right). \tag{13}$$

Case 4. When $\mu = 0$ and $\lambda \in \Re$,

$$\varphi(\xi) = \ln\left(\lambda(\xi + C)\right), \tag{14}$$

where C is defined as constant, $\lambda\mu < 0$, or $\lambda\mu > 0$ is conditional on the symbol of μ.

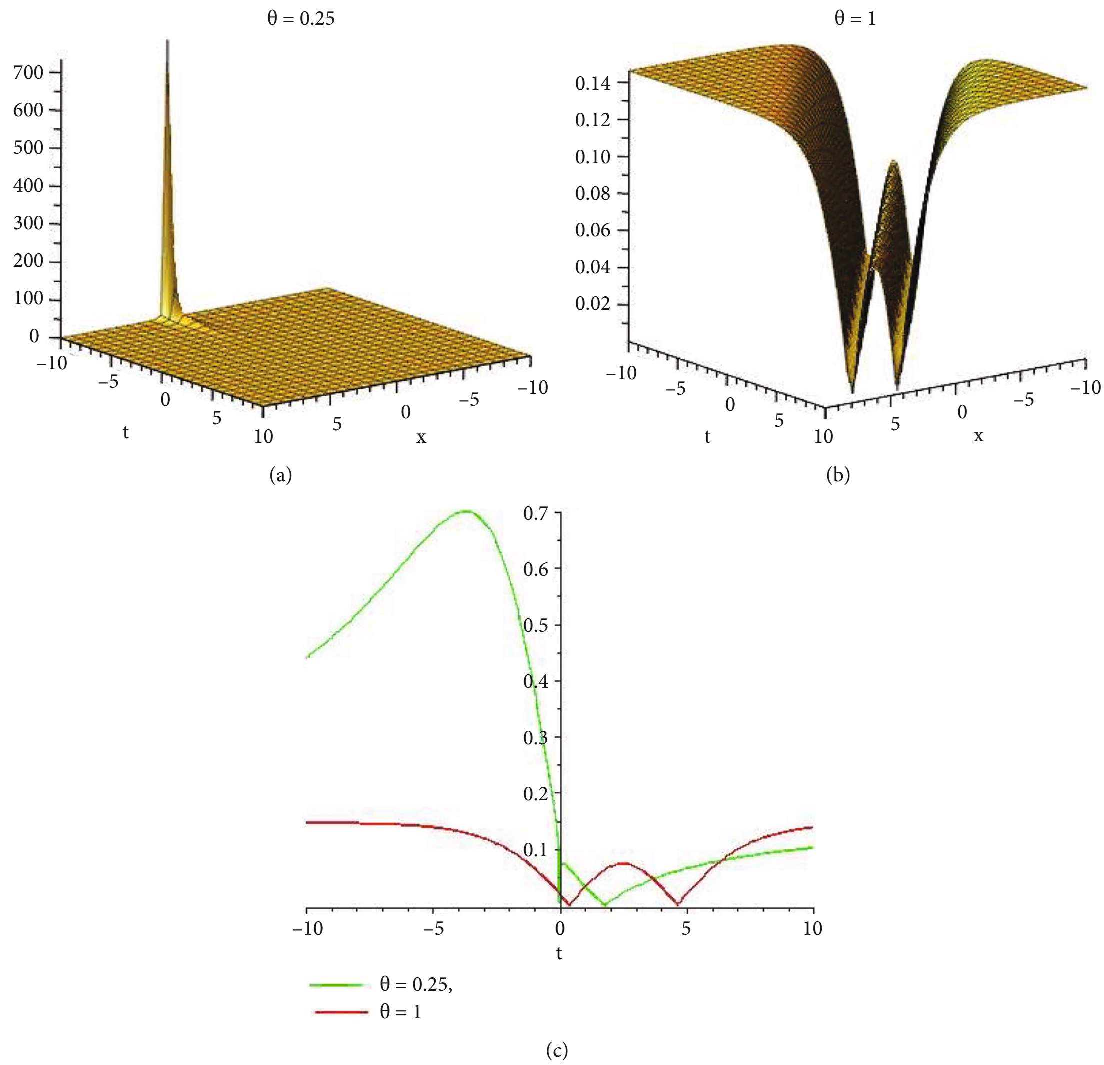

Figure 7: Dynamical behavior of function solution of $u_{8,9}(x, t)$. (a, b) 3D plot and (c) 2D combined plot for $x = 1$.

Step 3. By submitting Equation (9) into Equation (8) and finally consuming Equation (6), assemble all like term of order of $\exp(-q\varphi(\xi))$, $q = 0, \pm1, \pm2, \pm3, .. \cdots$ prearranged; then, we achieve a polynomial form of $\exp(-q\varphi(\xi))$ and connecting each coefficient of the gotten polynomial corresponding to zero, yields system of algebraic equations (SAE).

Step 4. Assume the constants' determination be attained as one or more results by determining the mathematical conditions in phase 3. Putting the constant designs laterally with the measures for Equation (7), from the evaluation equation, we can attain up-to-date, extensive, and exhaustive dynamic wave propagation (6).

4. Application of the Suggested Method

4.1. Application of $(2+1)$ CBS Equation. Consider the nonlinear time-fractional CBS equation in a conformable sense as follows (see, for example, [17]):

$$u_x N_t^{\theta} u + 4u_x u_{xy} + 2u_{xx} u_y + u_{xxxy} = 0, \quad t > 0 \text{ and } x, y \in R. \tag{15}$$

Here θ is a fractional parameter in a conformable sense with the interval $0 < \theta \leq 1$. Here $N_t^{\theta} u$ is conformable time fractional derivative of order θ. u_x and u_y are dispersive terms, where

$$u(x, y, t) = u(\xi), \quad \xi = x + y - w\frac{t^{\theta}}{\theta}. \tag{16}$$

Now using this voyaging wave variable $\xi = x + y - w(t^{\theta}/\theta)$ into Equation (15) and integrating with respect to ξ, we get the following transformation form of ordinary

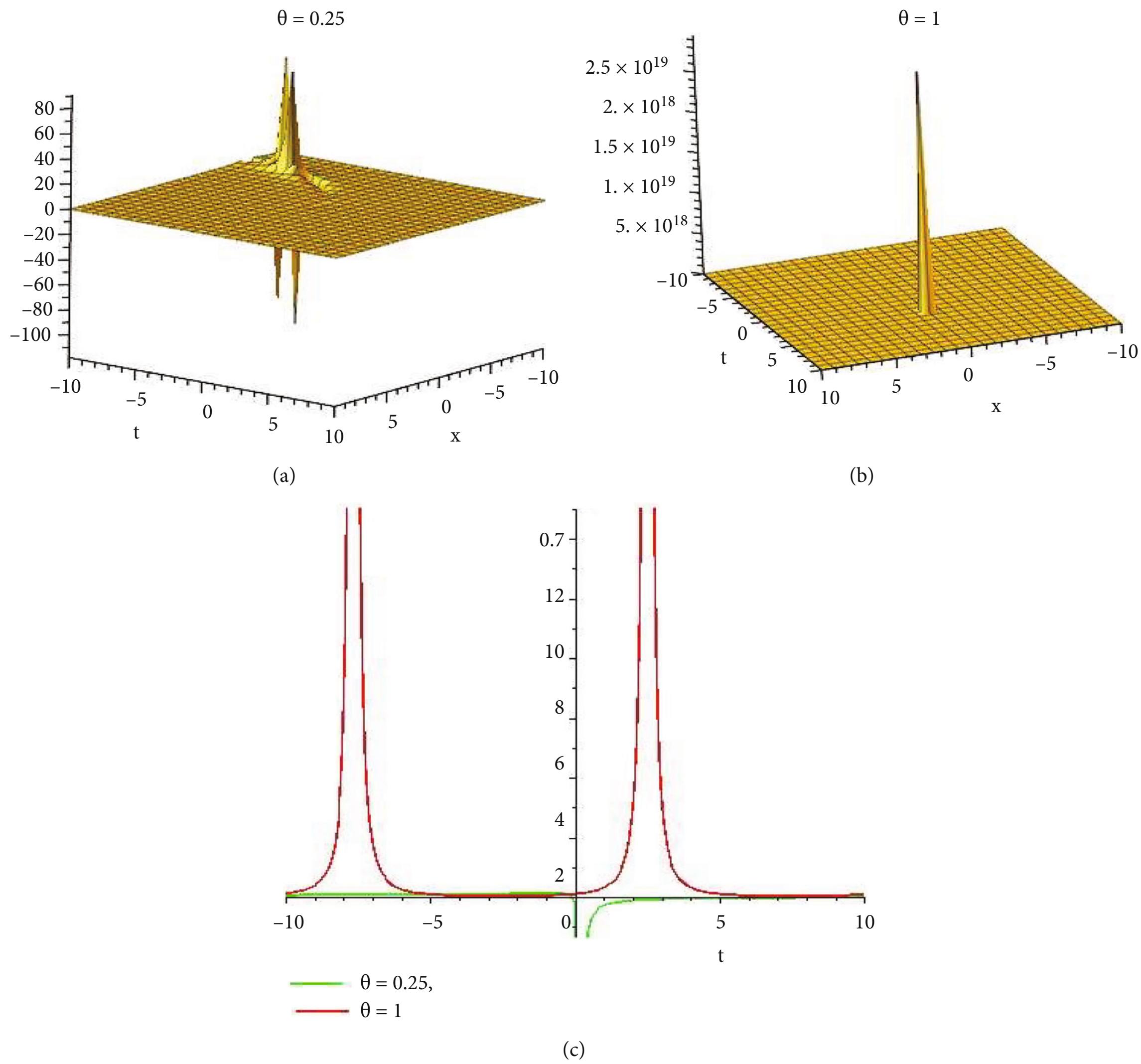

Figure 8: Dynamical behavior of function solution of $u_{10,11}(x, y, t)$. (a, b) 3D plot and (c) 2D combined plot for $x = 1$.

differential equations with the value $u = u(\xi)$.

$$-wu' + \left(\frac{\alpha+\beta}{2}\right)\left(u'\right)^2 + u''' = 0, \tag{17}$$

where primes indicate the differentiating with respect to ξ.

Now with the virtue of the homogeneous balancing method of u''' and $(u')^2$, we get the value of N as 1. As a result, Eq.(9) will term into the following form:

$$u(\xi) = A_0 + A_1 \exp\left(-\varphi(\xi)\right). \tag{18}$$

Hereafter differentiating Equation (18) regarding ξ and putting the value u, u', u''' into Equation (17), we obtain the same polynomial set.

Finally, equating the coefficients $e^{-i\phi(\xi)}$ equal to zero where $i = 0, \pm 1, \pm 2, \pm 3, \cdots\cdots$, we get some system of equations as follows.

$$\begin{aligned} &\frac{1}{2}{A_1}^2\beta\mu^2 + \frac{1}{2}{A_1}^2\alpha\mu^2 + wA_1\mu - 2A_1\lambda\mu^2 = 0, \\ &\alpha\lambda\mu {A_1}^2 + \beta\lambda\mu {A_1}^2 - 8\lambda^2\mu A_1 + \lambda w A_1 = 0, \\ &-6A_1\lambda^3 + \frac{1}{2}{A_1}^2\beta\lambda^2 + \frac{1}{2}{A_1}^2\alpha\lambda^2 = 0. \end{aligned} \tag{19}$$

Now solving the system of equations, we get one set of solutions.

Set 1

$$w = -4\lambda\mu, \quad A_0 = A_0, \quad A_1 = \frac{12\lambda}{\alpha+\beta}. \tag{20}$$

Case 1. When $\lambda\mu < 0$, the following solutions are obtained for hyperbolic functions:

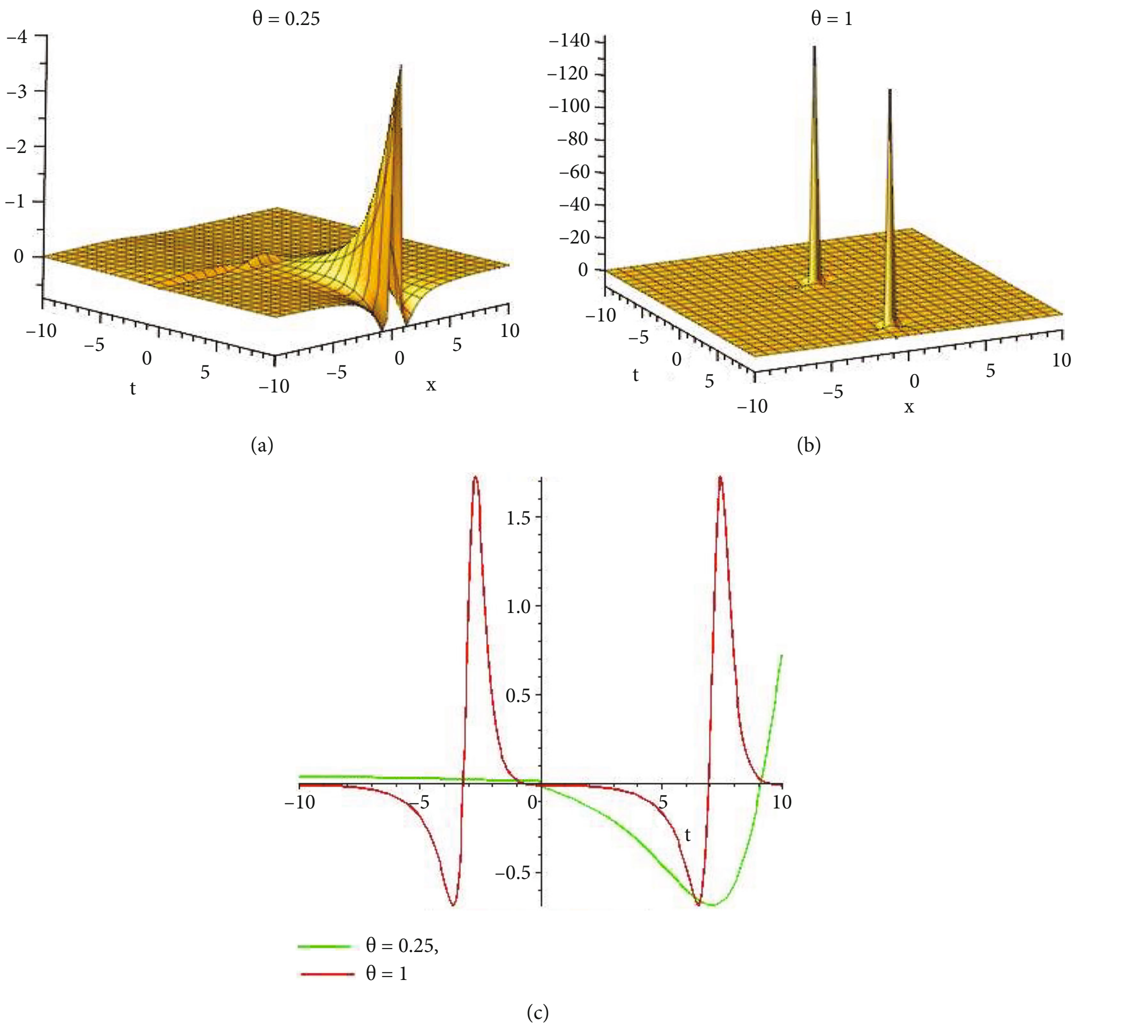

Figure 9: Dynamical behavior of function solution of $u_{12,13}(x, t)$. (a, b) 3D plot and (c) 2D combined stripe plot for $x = 1$.

Family 1

$$u_1(x, y, t) = \frac{A_0 + 12\lambda\left(\cosh\left(\sqrt{-\lambda\mu}\,\xi\right)\cosh\left(\sqrt{-\lambda\mu}C\right) + \sinh\left(\sqrt{-\lambda\mu}\xi\right)\sinh\left(\sqrt{-\lambda\mu}\,C\right)\right)}{(\alpha+\beta)\sqrt{-\lambda/\mu}\left(\sinh\left(\sqrt{-\lambda\mu}\,\xi\right)\cosh\left(\sqrt{-\lambda\mu}\,C\right) + \cosh\left(\sqrt{-\lambda\mu}\xi\right)\sinh\left(\sqrt{-\lambda\mu}\,C\right)\right)}, \tag{21}$$

where, $\xi = x + y + 4\lambda\mu w(t^\theta/\theta)$.

Family 2

$$u_2(x, y, t) = A_0 + \frac{12\lambda\left(\sinh\left(\sqrt{-\lambda\mu}\xi\right)\cosh\left(\sqrt{-\lambda\mu}C\right) + \cosh\left(\sqrt{-\lambda\mu}\xi\right)\sinh\left(\sqrt{-\lambda\mu}C\right)\right)}{(\alpha+\beta)\sqrt{-\lambda/\mu}\left(\cosh\left(\sqrt{-\lambda\mu}\xi\right)\cosh\left(\sqrt{-\lambda\mu}C\right) + \sinh\left(\sqrt{-\lambda\mu}\xi\right)\sinh\left(\sqrt{-\lambda\mu}C\right)\right)}, \tag{22}$$

where $\xi = x + y + 4\lambda\mu(t^\theta/\theta)$.

Case 2. The function solutions are trigonometric when $\lambda\mu > 0$.

Family 1

$$u_3(x,y,t) = A_0 + \frac{12\lambda}{(\alpha+\beta)\sqrt{\lambda/\mu}\left(\tan\left(\sqrt{\lambda\mu}C\right)+\tan\left(\sqrt{\lambda\mu}\xi\right)\right)} - \frac{12\lambda\left(\tan\left(\sqrt{\lambda\mu}C\right)\tan\left(\sqrt{\lambda\mu}\xi\right)\right)}{(\alpha+\beta)\sqrt{\lambda/\mu}\left(\tan\left(\sqrt{\lambda\mu}C\right)+\tan\left(\sqrt{\lambda\mu}\xi\right)\right)}, \tag{23}$$

where $\xi = x + y + 4\lambda\mu(t^\theta/\theta)$.

Family 2

$$u_4(x,y,t) = A_0 - \frac{12\lambda\cot\left(\sqrt{\lambda\mu}C\right)}{(\alpha+\beta)\sqrt{\lambda/\mu}\left(-1+\cot\left(\sqrt{\lambda\mu}C\right)\cot\left(\sqrt{\lambda\mu}\xi\right)\right)} - \frac{12\lambda\cot\left(\sqrt{\lambda\mu}\xi\right)}{(\alpha+\beta)\sqrt{\lambda/\mu}\left(-1+\cot\left(\sqrt{\lambda\mu}C\right)\cot\left(\sqrt{\lambda\mu}\xi\right)\right)}, \tag{24}$$

where $\xi = x + y + 4\lambda\mu(t^\theta/\theta)$.

Case 3. When $\mu > 0$ and $\lambda = 0$, the solution is not sufficient, so we can neglect this case.

Case 4. $u_5(x,y,t) = A_0 + 12/(\alpha+\beta)(\xi + C)$, where, $\xi = x + y$ and C is an arbitrary constant.

4.2. Application of RLW Equation. In this section, we applied our mentioned method to the time-fractional RLW equation as follows [31].

$$N_t{}^\theta u + u_x + \alpha\left(u^2\right)_x - \beta u_{xx} N_t{}^\theta u = 0, \quad t > 0 \text{ and } x, y \in R. \tag{25}$$

Here θ is the fractional constant with the interval $0 < \theta \le 1$, where

$$u(x,t) = u(\xi), \quad \xi = mx + n\frac{t^\theta}{\theta}. \tag{26}$$

By utilizing this wave variable of Equation (26) into Equation (25) and integrating with respect to ξ, we get this ordinary differential equation form.

$$(n+m)\,u + \alpha u^2 - \beta m^2 n^2 u'' = 0, \tag{27}$$

where u' represents the differentiating of u with respect to ξ.

With the homogeneous balancing of the highest order nonlinear term u^2 and the highest linear term u'', we find the value of $N2$. As an outcome, ?added value=" Eq.(9)"?>can be written in the following form.

$$u(\xi) = A_0 + A_1(-\varphi(\xi)) + A_2\{(-\varphi(\xi))\}^2. \tag{28}$$

Hereafter, we differentiate Equation (28) regarding ξ and putting the required value u, u^2, u'' in Eq.(17).

Therefore, we finally get some polynomials and equate the coefficients $e^{-i\phi(\xi)}$ equal to zero, where $i = 0, \pm1, \pm2, \pm3, \cdots\cdots$, and we get some system of equations as follows.

$$\begin{gathered}
-2\beta m^2 n^2 A_2 \mu^2 + \alpha A_0{}^2 + mA_0 + nA_0 = 0, \\
-2\beta\lambda m^2 \mu n^2 A_1 + 2\alpha A_0 A_1 + mA_1 + nA_1 = 0, \\
-8\beta\lambda m^2 \mu n^2 A_2 + 2\alpha A_0 A_2 + \alpha A_1{}^2 + mA_2 + nA_2 = 0, \\
-2\beta\lambda^2 m^2 n^2 A_1 + 2\alpha A_1 A_2 = 0, \\
-6\beta\lambda^2 m^2 n^2 A_2 + \alpha A_2{}^2 = 0.
\end{gathered} \tag{29}$$

Now by solving this system of equations, we find two sets of solutions as below.

Set 1

$$\begin{gathered}
m = \pm\frac{1}{8}\frac{\pm1 + \sqrt{16\beta n\lambda\mu n^2 + 1}/\beta\lambda\mu n^2}{\alpha}, \\
m = n, \\
A_0 = \frac{1}{2}\frac{\pm1/8\left(\pm1 + \sqrt{16\beta n\lambda\mu n^2 + 1}/\beta\lambda\mu n^2\right) + n}{\alpha}, \\
A_1 = 0, \\
A_2 = \frac{3}{2}\frac{\left(\pm1/8\left(\pm1 + \sqrt{16\beta n^3\lambda\mu + 1}/\beta\lambda\mu n^2\right) + n\right)\lambda}{\mu\alpha}.
\end{gathered} \tag{30}$$

Set 2

$$\begin{gathered}
m = \pm\frac{1}{8}\frac{\pm1 + \sqrt{-16\beta n\lambda\mu n^2 + 1}/\beta\lambda\mu n^2}{\alpha}, \\
A_0 = -\frac{3}{2}\frac{\pm1/8\left(\pm1 + \sqrt{-16\beta n^3\mu\lambda + 1}/\beta\lambda\mu n^2\right) + n}{\alpha}, \\
A_2 = -\frac{3}{2}\frac{\left(\pm1/8\left(\pm1 + \sqrt{-16\beta n\lambda n^2 + 1}/\beta\lambda\mu n^2\right) + n\right)\lambda}{\mu\alpha}.
\end{gathered} \tag{31}$$

Case 1. when $\lambda\mu < 0$, the following solutions are obtained for hyperbolic functions:

Set 1.

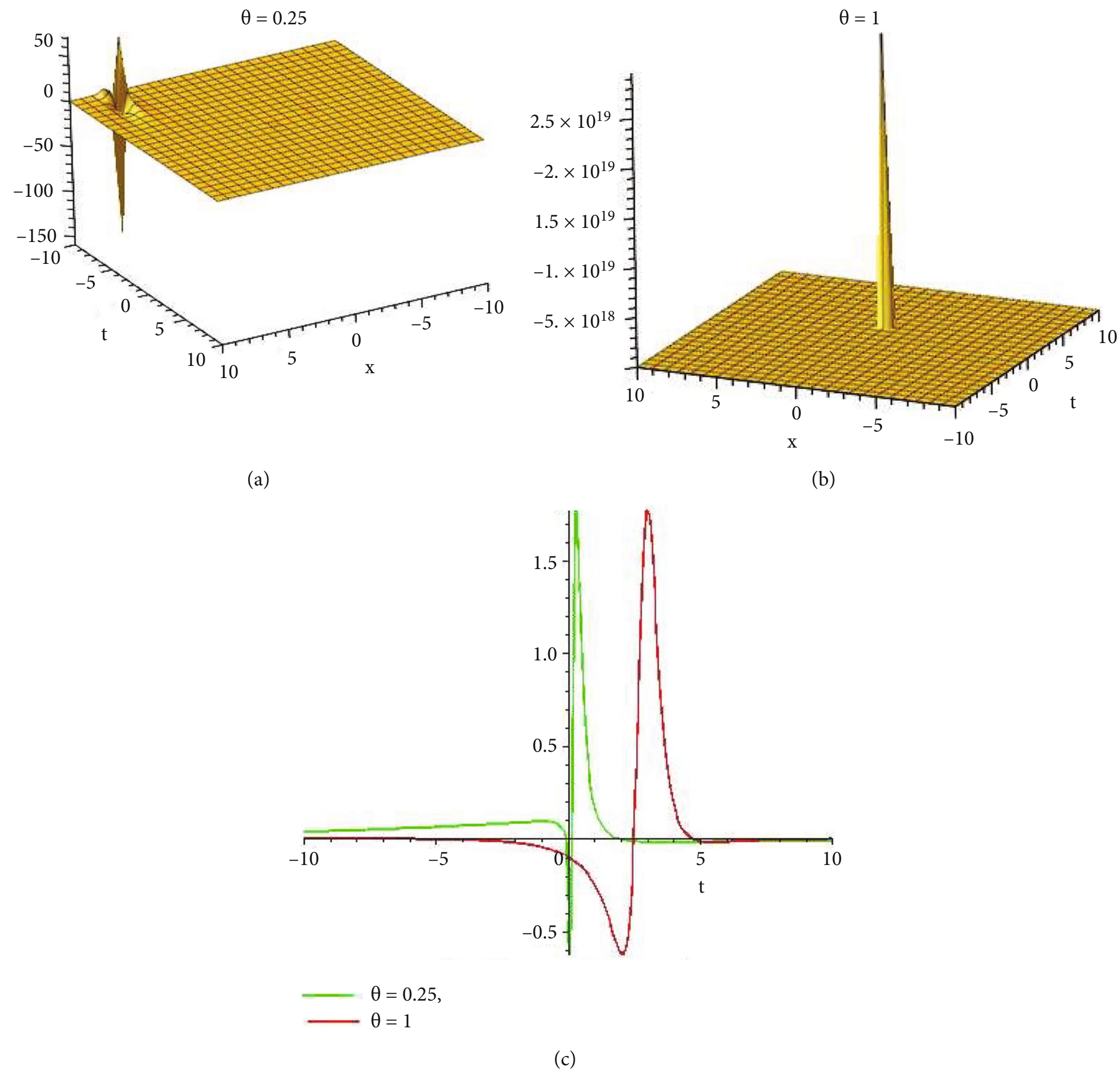

Figure 10: Dynamical behavior of function solution of $u_{14,15}(x,t)$. (a, b) 3D plot and (c) 2D combined plot for $x = 1$.

Family 1

$$u_{6,7}(x,t) = \frac{1}{2}\frac{\pm 1/8\left(\pm 1 + \sqrt{16\beta\lambda\mu n^3 + 1}/\beta\lambda\mu n^2 + n\right.}{\alpha} + \frac{A_1}{\sqrt{-\lambda/\mu}\tanh\left(\sqrt{-\lambda\mu}(\xi + C)\right)} - \frac{3}{2}\frac{\pm 1/8\left(\pm 1 + \sqrt{16\beta\lambda\mu n^3 + 1}/\beta\lambda\mu n^2\right) + n}{\alpha\tanh\left(\sqrt{-\lambda\mu}(\xi + C)\right)^2}, \tag{32}$$

where $\xi = \pm 1/8(\pm 1 + \sqrt{16\beta\lambda\mu n^3 + 1}/\beta\lambda\mu n^2)x + n(t^\theta/\theta)$.

Family 2

$$\xi = \pm\frac{1}{8}\frac{\pm 1 + \sqrt{16\beta\lambda\mu n^3 + 1}}{\beta\lambda\mu n^2}x + n\frac{t^\theta}{\theta}.\xi = \pm\frac{1}{8}\frac{\pm 1 + \sqrt{16\beta\lambda\mu n^3 + 1}}{\beta\lambda\mu n^2}x + n\frac{t^\theta}{\theta},$$

$$u_{8,9}(x,t) = \frac{1}{2}\frac{\pm 1/8\left(\pm 1 + \sqrt{16\beta\lambda\mu n^3 + 1}/\beta\lambda\mu n^2\right) + n}{\alpha} + \frac{A_1}{\sqrt{-\lambda/\mu}\coth\left(\sqrt{-\lambda\mu}(\xi + C)\right)} - \frac{3}{2}\frac{\pm 1/8\left(\pm 1 + \sqrt{16\beta\lambda\mu n^3 + 1}/\beta\lambda\mu n^2\right) + n}{\alpha\coth\left(\sqrt{-\lambda\mu}(\xi + C)\right)^2}, \tag{33}$$

where $\xi = \pm 1/8(\pm 1 + \sqrt{16\beta\lambda\mu n^3 + 1}/\beta\lambda\mu n^2)x + n(t^\theta/\theta)$.

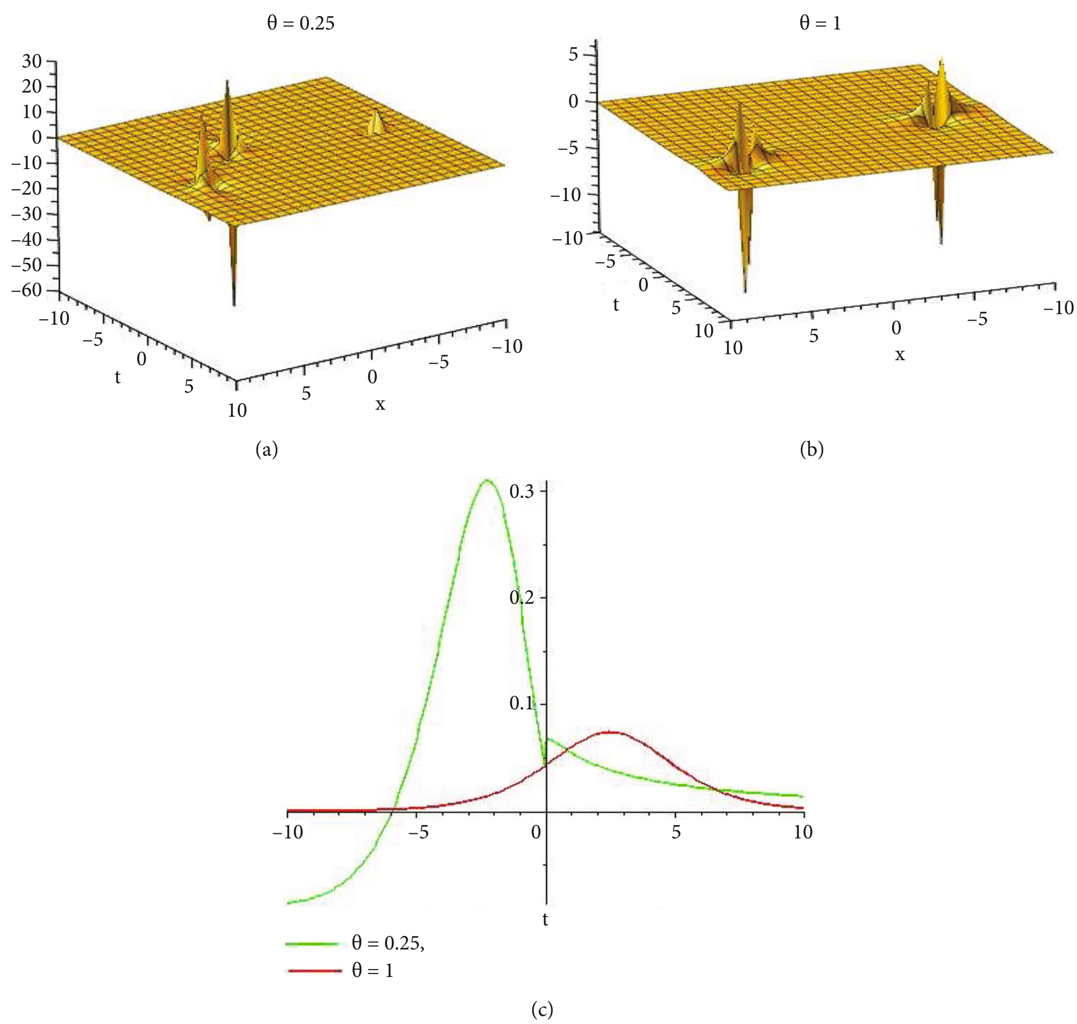

FIGURE 11: Dynamical behavior of function solution of $u_{16,17}(x,t)$. (a, b) 3D plot and (c) 2D combined stripe plot for $x=1$.

Set 2
Family 1

$$u_{10,11}(x,t) = -\frac{3}{2}\frac{\pm 1/8\left(\pm 1 + \sqrt{-16\beta\lambda\mu n^3 + 1}/\beta\lambda\mu n^2\right) + n}{\alpha} + \frac{A_1}{\sqrt{-\lambda/\mu}\tanh\left(\sqrt{-\lambda\mu}(\xi + C)\right)} + \frac{3}{2}\frac{\pm 1/8\left(\pm 1 + \sqrt{-16\beta\lambda\mu n^3 + 1}/\beta\lambda\mu n^2\right) + n}{\alpha\tanh\left(\sqrt{-\lambda\mu}(\xi + C)\right)^2}, \quad (34)$$

where $\xi = \pm 1/8(\pm 1 + \sqrt{16\beta\lambda\mu n^3 + 1}/\beta\lambda\mu n^2)x + n(t^{\theta}/\theta)$.

Family 2

$$u_{12,13}(x,t) = -\frac{3}{2}\frac{\pm 1/8\left(\pm 1 + \sqrt{-16\beta\lambda\mu n^3 + 1}/\beta\lambda\mu n^2\right) + n}{\alpha} + \frac{A_1}{\sqrt{-\lambda/\mu}\coth\left(\sqrt{-\lambda\mu}(\xi + C)\right)} + \frac{3}{2}\frac{\pm 1/8\left(\pm 1 + \sqrt{-16\beta\lambda\mu n^3 + 1}/\beta\lambda\mu n^2\right) + n}{\alpha\coth\left(\sqrt{-\lambda\mu}(\xi + C)\right)^2}, \quad (35)$$

where $\xi = \pm 1/8(\pm 1 + \sqrt{16\beta\lambda\mu n^3 + 1}/\beta\lambda\mu n^2)x + n(t^{\theta}/\theta)$.

Case 2. The function solutions are trigonometric when $\lambda\mu > 0$.

Set 1

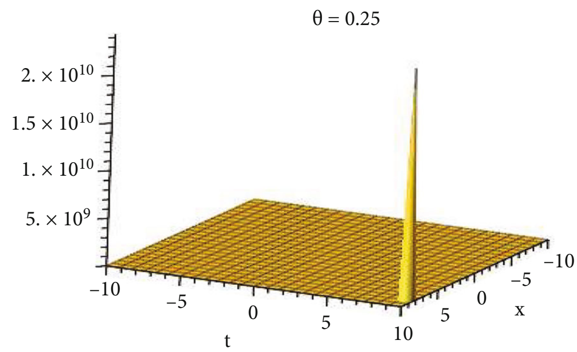

(a)

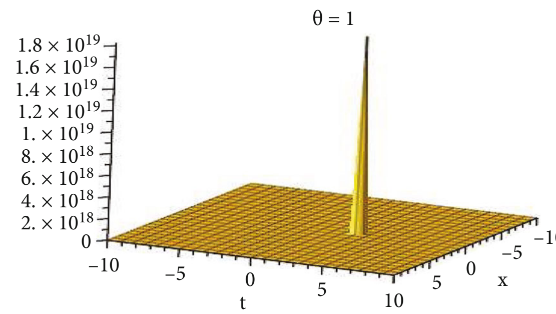

(b)

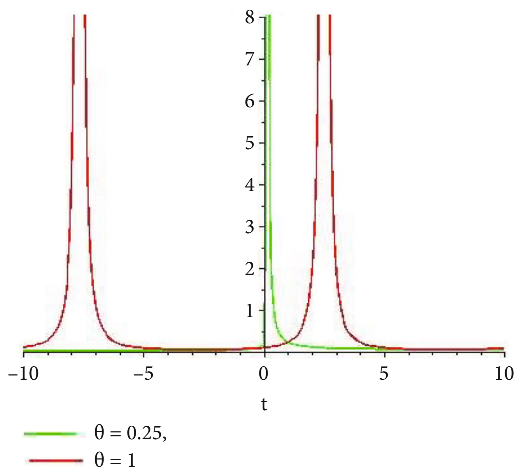

(c)

Figure 12: Dynamical behavior of function solution of $u_{18,19}(x, y, t)$. (a, b) 3D plot view representation and (c) 2D combined plot for $x = 1$, respectively.

Family 1

$$u_{14,15}(x,t) = \frac{1}{2}\frac{\pm 1/8\left(\pm 1 + \sqrt{16\beta\,\lambda\mu\, n^3 + 1}/\beta\,\lambda\mu\, n^2\right) + n}{\alpha} + \frac{A_1}{\sqrt{\lambda/\mu}\tan\left(\sqrt{\lambda\mu}(\xi + C)\right)} + \frac{3}{2}\frac{\pm 1/8\left(\pm 1 + \sqrt{16\beta\,\lambda\mu\, n^3 + 1}/\beta\,\lambda\mu\, n^2\right) + n}{\alpha\tan\left(\sqrt{\lambda\mu}(\xi + C)\right)^2}, \quad (36)$$

where $\xi = \pm 1/8(\pm 1 + \sqrt{16\beta\,\lambda\mu\, n^3 + 1}/\beta\,\lambda\mu\, n^2)x + n(t^\theta/\theta)$

.

Family 2

$$u_{16,17}(x,t) = \frac{1}{2}\frac{\pm 1/8\left(\pm 1 + \sqrt{16\beta\,\lambda\mu\, n^3 + 1}/\beta\,\lambda\mu\, n^2\right) + n}{\alpha} - \frac{A_1}{\sqrt{\lambda/\mu}\cot\left(\sqrt{\lambda\mu}(\xi + C)\right)} + \frac{3}{2}\frac{\pm 1/8\left(\pm 1 + \sqrt{16\beta\,\lambda\mu\, n^3 + 1}/\beta\,\lambda\mu\, n^2\right) + n}{\alpha\cot\left(\sqrt{\lambda\mu}(\xi + C)\right)^2}, \quad (37)$$

where $\xi = \pm 1/8(\pm 1 + \sqrt{16\beta\,\lambda\mu\, n^3 + 1}/\beta\,\lambda\mu\, n^2)x + n(t^\theta/\theta)$.

Set 2

Family 1

$$u_{18,19}(x,t) = -\frac{3}{2}\frac{\pm 1/8\left(\pm 1 + \sqrt{-16\beta\,\lambda\mu\, n^3 + 1}/\beta\,\lambda\mu\, n^2\right) + n}{\alpha} + \frac{A_1}{\sqrt{\lambda/\mu}\tan\left(\sqrt{\lambda\mu}(\xi + C)\right)} - \frac{3}{2}\frac{\pm 1/8\left(\pm 1 + \sqrt{-16\beta\,\lambda\mu\, n^3 + 1}/\beta\,\lambda\mu\, n^2\right) + n}{\alpha\tan\left(\sqrt{\lambda\mu}(\xi + C)\right)^2}, \quad (38)$$

where $\xi = \pm 1/8(\pm 1 + \sqrt{-16\beta\,\lambda\mu\, n^3 + 1}/\beta\,\lambda\mu\, n^2)x + n(t^\theta/\theta)$.

Family 2

$$u_{20,21}(x,t) = -\frac{3}{2}\frac{\pm 1/8\left(\pm 1 + \sqrt{-16\beta\,\lambda\mu\, n^3 + 1}/\beta\,\lambda\mu\, n^2\right) + n}{\alpha} - \frac{A_1}{\sqrt{\lambda/\mu}\cot\left(\sqrt{\lambda\mu}(\xi + C)\right)} - \frac{3}{2}\frac{\pm 1/8\left(\pm 1 + \sqrt{-16\beta\,\lambda\mu\, n^3 + 1}/\beta\,\lambda\mu\, n^2\right) + n}{\alpha\cot\left(\sqrt{\lambda\mu}(\xi + C)\right)^2}, \quad (39)$$

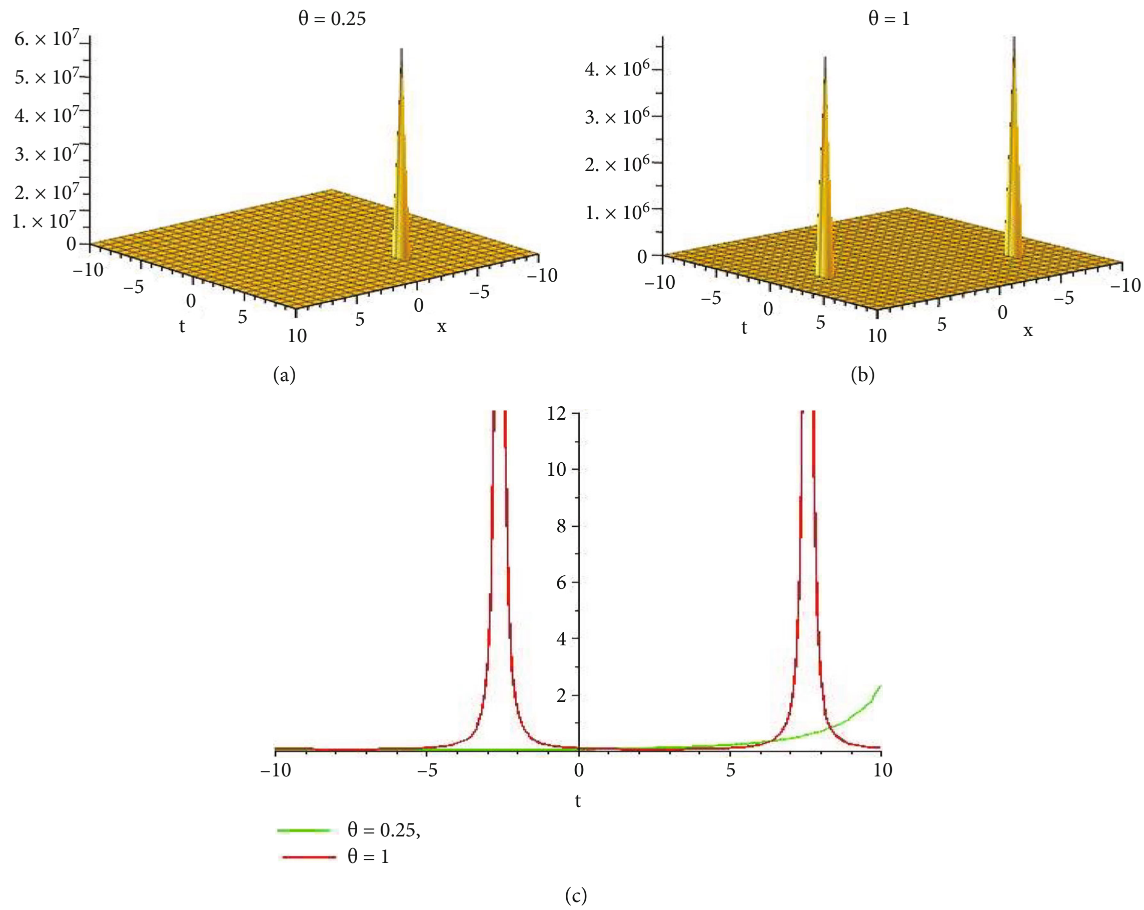

Figure 13: Dynamical behavior of function solution of $u_{20,21}(x, t)$. (a, b) 3D plot and (c) 2D combined plot for $x = 1$.

where $\xi = \pm 1/8(\pm 1 + \sqrt{-16\beta\lambda\mu n^3 + 1}/\beta\lambda\mu n^2)x + n(t^\theta/\theta)$.

5. Results and Discussion

Physical and graphical representation of newly established solutions of the $(2+1)$-dimensional CBS and RLW equation will be well-defined in this segment. Pictorial representation is the absolute means of envisioning the complete tangible sense of real-life concerns. We also showed the graphical depiction of our resultant solutions exhausting the computational Maple features to designate the fractional-order derivative by selecting suitable fractional values of θ. We have assigned specific high costs to the unidentified parameters to envision the consequent solutions' natural features. The established equations are presented in Figures 1–13, which have been designed.

5.1. Physical Explanation. This subsection will focus on the physical elucidation of the $(2+1)$-dimensional CBS and RLW equation exact solutions by utilizing the advanced $\exp(-\varphi(\xi))$-expansion scheme. The attained solutions $u_1(x, y, t)$, $u_2(x, y, t)$, , $u_{8,9}(x, t)$, $u_{10,11}(x, t)$, and $u_{12,13}(x, t)$ are hyperbolic function solutions, $u_3(x, y, t)$, $u_4(x, y, t)$, $u_{14,15}(x, t)$, $u_{6,7}(x, t)u_{16,17}(x, t)$, $u_{18,19}(x, t)$, and $u_{20,21}(x, t)$ are trigonometric function solutions, and $u_5(x, t)$ is an algebraic solution. Figures 1–5 are presented from CBS equation. Figures 6–13 are from the RLW equation. In every set of figures, we have changed the free parameter of our preferred equation and fractional-order derivative $\theta = 0.25$ to 1 with other suitable parameters to show the dynamical behavior of attained solutions. Figure 1 represents the singular soliton shape $u_1(x, y, t)$ for the fractional value $\theta = 0.25$ with the suitable parameters $\lambda = 3$, $\mu = -2$, $C = -0.5$, $A = 1$, $\alpha = 1$, and $\beta = 1$; with the change of fractional parameter, $\theta = 0.25$ to 1, the solution shape changes its amplitude and size only, but there have no changes for the variety of free parameters α and β. Figure 2 represents the bright soliton solution shape $u_2(x, y, t)$ for the fractional value $\theta = 0.25$ with the suitable parameters $\lambda = 3$, $\mu = -2$, $C = -0.5$, $A = 1$, $\alpha = 1$, and $\beta = 1$. With the change of fractional parameter, $\theta = 0.25$ to 1, the solution shape turns into the dark soliton shape. Here for the evolution of free parameters α and β, the solution shape changes its amplitude and size only. Figures 3 and 4 represent the periodic singular solution shape $u_3(x, y, t)$ and $u_4(x, y, t)$ for the fractional value $\theta = 0.25$ with the suitable parameters. With the variety of fractional parameters $\theta = 0.25$ to 1 and free parameters, the solution has no dynamical change but only its amplitude and size. Figure 5 represents the singular soliton solution shape $u_5(x, y, t)$ for the fractional value $\theta = 0.25$ with the suitable parameters $\lambda = 2$, $\mu = 0$, $C = -0.5$, $A = 1$, $\alpha = 1$, and $\beta = 1$. With the variety of fractional parameters $\theta = 0.25$ to 1 and free parameters, the solution has no dynamical change. Figures 6–9 belong to the set-1 solution set, and Figures 10–13 belong to the set-2 solution set of the RLW equation. Figure 6 represents the two soliton solution shape of $u_6(x, t)$ for the fractional value $\theta = 0.25$ with the suitable parameters $\lambda = 3$, $\mu = -0.2$, $C = -0.5$, $n = -0.4$, $\alpha = 6$, and $\beta = 10$. With the variety of fractional parameters, $\theta = 0.25$ to 1, the two-soliton shape turns into the one-soliton shape and has no change with free parameters. Figure 7 represents the one-soliton solution shape $u_7(x, t)$ for the fractional value $\theta = 0.25$ with the right parameters $\lambda = 3$, $\mu = -0.2$, $C = -0.5$, $n = -0.4$, $\alpha = 6$, and $\beta = 10$. Shape moves to W-shaped solution shape for the transformation of fractional-order derivative $\theta = 0.25$ to 1. Herewith, with the change of free parameters α and β, the solution shape changes its amplitude and size only. Figures 8 and 9 represent the singular soliton shape of $u_{14,15}(x, t)$ and $u_{16,17}(x, t)$ for the fractional value $\theta = 0.25$ with the suitable parameters $\lambda = 3$, $\mu = -0.2$, $C = -0.5$, $n = -0.4$, $\alpha = 6$, and $\beta = 10$. With the variety of fractional parameters, $\theta = 0.25$ to 1, the singular soliton shape turns into the two-soliton shape and has no change with free parameters. Figure 10 represents the rogue wave soliton shape $u_{10,11}(x, t)$ for the fractional value $\theta = 0.25$ with the suitable parameters $\lambda = 3$, $\mu = -0.2$, $C = 1$, $n = -0.4$, $\alpha = 6$, and $\beta = 10$. With the variety of fractional parameter, $\theta = 0.25$ to 1, the rogue wave turns into the singular soliton shape. Figure 11 represents the rogue wave soliton shape $u_{12,13}(x, t)$ for the fractional value $\theta = 0.25$ with the suitable parameters $\lambda = 3$, $\mu = -0.2$, $C = 1$, $n = -0.4$, $\alpha = 6$, and $\beta = 10$. With the variety of fractional parameter, $\theta = 0.25$ to 1, the rogue wave changes its amplitude and size only. Figures 12 and 13 represent the singular soliton shape of $u_{18,19}(x, t)$ and $u_{20,21}(x, t)$ for the fractional value $\theta = 0.25$ with the suitable parameters $\lambda = 3$, $\mu = -0.2$, $C = 1$, $n = -0.4$, $\alpha = 6$, and $\beta = 10$. With the variety of fractional parameters, $\theta = 0.25$ to 1, the singular soliton shape turns into the two-soliton shape.

5.2. Graphical Representation. The graphical decorations of our attained solutions of the $(2 + 1)$-dimensional CBS and RLW equation have exposed in this subsection. Our preferred equations are resolved, and attained solutions are extracted from the trigonometric and hyperbolic function by computational tool Maple 21. For detailed physical clarity, all precise solution charts are exhibited in 3D as well as 2D combined stripe charts.

6. Conclusions

In the above study, exact wave solutions with several types of wave constructions for time fractional $(2 + 1)$-dimensional CBS and RLW equation have been accumulated through the advanced exp $(-\varphi(\xi))$ expansion technique. The dissimilar wave structures characterized the attained solutions' dynamical behavior in this system. Preferred fractional and free parameters have significant insinuations, such as putting the dissimilar magnitude of the fractional and free parameters from a separate function of meaningful solutions can be originated exclusively and variation of suitable parameters has a significant impact on the wave. Moreover, we claim that our obtained traveling solutions are new in the sense of conformable derivative and could be operative in the research of nonlinear physical phenomena. It is very clear to decide that our promoted technique is effective, reliable, and friendly applicable and delivers sufficient well-matched explanations to NLFEEs arise in engineering, applied mathematics, nonlinear dynamics, and mathematical physics.

Data Availability

All required data were included in the manuscript and cited appropriately when it was required.

Conflicts of Interest

The authors declare that they have no conflicts of interest.

Acknowledgments

The authors like to express their gratitude to the Bangladesh University of Engineering and Technology (BUET), Bangladesh, for providing financial support under the Basic Research Grant No. 1111202109017. The second author (Foyjonnesa) specially wants to express her deepest gratitude to the Bangladesh University of Engineering and Technology (BUET), for selecting her as a PG Fellow (Ph.D. Mathematics).

References

[1] H. L. Zhen, B. Tian, Y. F. Wang, and D. Y. Liu, "Soliton solutions and chaotic motions of the Zakharov equations for the Langmuir wave in the plasma," *Physics of Plasmas*, vol. 22, no. 3, article 032307, 2015.

[2] R. Hayward and F. Biancalana, "Constructing new nonlinear evolution equations with supersymmetry," *Journal of Physics A: Mathematical and Theoretical*, vol. 51, no. 27, article 275202, 2018.

[3] C. T. Sendi, J. Manafian, H. Mobasseri, M. Mirzazadeh, Q. Zhou, and A. Bekir, "Application of the ITEM for solving three nonlinear evolution equations arising in fluid mechanics," *Nonlinear Dynamics*, vol. 95, no. 1, pp. 669–684, 2019.

[4] X. Y. Xie, B. Tian, W. R. Sun, M. Wang, and Y. P. Wang, "Solitary wave and multi-front wave collisions for the Bogoyavlenskii–Kadomtsev–Petviashili equation in physics, biology and electrical networks," *Modern Physics Letters B*, vol. 29, no. 31, p. 1550192, 2015.

[5] H. O. Roshid and W. X. Ma, "Dynamics of mixed lump-solitary waves of an extended (2+1)-dimensional shallow water wave model," *Physics Letters A*, vol. 382, no. 45, pp. 3262–3268, 2018.

[6] M. B. Hossen, H. O. Roshid, and M. Z. Ali, "Characteristics of the solitary waves and rogue waves with interaction phenomena in a (2+1)-dimensional breaking soliton equation," *Physics Letters A*, vol. 382, no. 19, pp. 1268–1274, 2018.

[7] A. A. Mamun, N. H. M. Shahen, S. N. Ananna, M. Asaduzzaman, and Foyjonnesa, "Solitary and periodic

wave solutions to the family of new 3D fractional WBBM equations in mathematical physics," *Heliyon*, vol. 7, no. 7, article e07483, 2021.

[8] J. Manafian and N. Allahverdiyeva, "An analytical analysis to solve the fractional differential equations," *Advanced Mathematical Models & Application*, vol. 6, no. 2, pp. 128–161, 2021.

[9] F. Meng and Q. Feng, "Exact solutions with variable coefficient function forms for conformable fractional partial differential equations by an auxiliary equation method," *Advances in Mathematical Physics*, vol. 2018, Article ID 4596506, 8 pages, 2018.

[10] S. T. Demiray and S. Duman, "MTEM to the $(2+1)$-dimensional ZK equation and Chafee-Infante equation," *Advanced Mathematical Models & Applications*, vol. 6, no. 1, pp. 63–70, 2021.

[11] N. H. M. Shahen, Foyjonnesa, M. H. Bashar, M. S. Ali, and A. A. Mamun, "Dynamical analysis of long-wave phenomena for the nonlinear conformable space-time fractional (2+1)-dimensional AKNS equation in water wave mechanics," *Heliyon*, vol. 6, no. 10, article e05276, 2020.

[12] J. Manafian and M. Lakestani, "Abundant soliton solutions for the Kundu–Eckhaus equation via $\tan(\phi(\xi))$-expansion method," *Optik*, vol. 127, no. 14, pp. 5543–5551, 2016.

[13] Z. Rahman, M. Z. Ali, and H. O. Roshid, "Closed form soliton solutions of three nonlinear fractional models through proposed improved Kudryashov method," *Chinese Physics B*, vol. 30, no. 5, article 050202, 2021.

[14] F. Ferdous, M. G. Hafez, and M. Y. Ali, "Obliquely propagating wave solutions to conformable time fractional extended Zakharov–Kuzetsov equation via the generalized $\exp(-\Phi(\xi))$-expansion method," *SeMA Journal*, vol. 76, no. 1, pp. 109–122, 2019.

[15] M. M. A. Khater, "Exact traveling wave solutions for the generalized Hirota-Satsuma couple KdV system using the exp $(-\varphi(\xi))$-expansion method," *Cogent Mathematics*, vol. 3, no. 1, p. 1172397, 2016.

[16] M. G. Hafez and D. Lu, "Traveling wave solutions for space-time fractional nonlinear evolution equations," 2015, https://arxiv.org/abs/1512.00715.

[17] H. C. Yaslan and A. Girgin, "New exact solutions for the conformable space-time fractional KdV, CDG, $(2+1)$-dimensional CBS and $(2+1)$-dimensional AKNS equations," *Journal of Taibah University for Science*, vol. 13, no. 1, pp. 1–8, 2019.

[18] M. M. Rahhman, A. Aktar, and K. C. Roy, "Analytical solutions of nonlinear coupled Schrodinger–KdV equation via advance exponential expansion," *American Journal of Mathematical and Computer Modelling*, vol. 3, no. 3, pp. 46–51, 2018.

[19] A. M. Wazwaz, "Erratum to:"Multiple-soliton solutions for the ninth-order KdV equation and sixth-order Boussinesq equation"[Appl. Math. Comput. 203 (2008) 277–283]," *Applied Mathematics and Computation*, vol. 206, no. 2, p. 1005, 2008.

[20] Y. Z. Peng, "New types of localized coherent structures in the Bogoyavlenskii-Schiff equation," *International Journal of Theoretical Physics*, vol. 45, no. 9, pp. 1764–1768, 2006.

[21] T. Kobayashi and K. Toda, "Methods and applications," *Symmetry, Integrability and Geometry: Methods and Applications*, vol. 2, p. 1, 2006.

[22] A. M. Wazwaz, "The $(2+1)$ and $(3+1)$-dimensional CBS equations: multiple soliton solutions and multiple singular soliton solutions," *Zeitschrift für Naturforschung A*, vol. 65, no. 3, pp. 173–181, 2010.

[23] M. S. Bruzón, M. L. Gandarias, C. Muriel, J. Ramirez, S. Saez, and F. R. Romero, "The Calogero–Bogoyavlenskii–Schiff equation in $2+1$ dimensions," *Theoretical and Mathematical Physics*, vol. 137, no. 1, pp. 1367–1377, 2003.

[24] J. M. Wang and X. Yang, "Quasi-periodic wave solutions for the (2+1)-dimensional generalized Calogero–Bogoyavlenskii–Schiff (CBS) equation," *Nonlinear Analysis: Theory, Methods & Applications*, vol. 75, no. 4, pp. 2256–2261, 2012.

[25] A. M. Wazwaz, "Negative-order forms for the Calogero–Bogoyavlenskii–Schiff equation and the modified Calogero–Bogoyavlenskii–Schiff equation," *Proceedings of the Romanian Academy, Series A*, vol. 18, no. 4, pp. 337–344, 2017.

[26] R. Saleh, M. Kassem, and S. Mabrouk, "Exact solutions of Calgero-Bogoyavlenskii-Schiff equation using the singular manifold method after Lie reductions," *Mathematical Methods in the Applied Sciences*, vol. 40, no. 16, pp. 5851–5862, 2017.

[27] M. O. Al-Amr, "Exact solutions of the generalized $(2+1)$-dimensional nonlinear evolution equations via the modified simple equation method," *Computers & Mathematics with Applications*, vol. 69, no. 5, pp. 390–397, 2015.

[28] A. M. Wazwaz, "Abundant solutions of various physical features for the $(2+1)$-dimensional modified KdV-Calogero–Bogoyavlenskii–Schiff equation," *Nonlinear Dynamics*, vol. 89, no. 3, pp. 1727–1732, 2017.

[29] P. Nithiarasu, R. Codina, and O. C. Zienkiewicz, "The Characteristic-Based Split (CBS) scheme—a unified approach to fluid dynamics," *International Journal for Numerical Methods in Engineering*, vol. 66, no. 10, pp. 1514–1546, 2006.

[30] M. Shakeel and S. T. Mohyud-Din, "Improved (G'/G)-expansion and extended tanh methods for (2+1)-dimensional Calogero–Bogoyavlenskii–Schiff equation," *Alexandria Engineering Journal*, vol. 54, no. 1, pp. 27–33, 2015.

[31] H. Aminikhah, A. H. Refahi Sheikhani, and H. Rezazadeh, "Sub-equation method for the fractional regularized long-wave equations with conformable fractional derivatives," *Scientia Iranica*, vol. 23, no. 3, pp. 1048–1054, 2016.

[32] B. Fornberg and G. B. Whitham, "A numerical and theoretical study of certain nonlinear wave phenomena," *Philosophical transactions of the Royal Society of London. Series A, Mathematical and Physical Sciences*, vol. 289, no. 1361, pp. 373–404, 1978.

[33] H. N. Hassan and H. K. Saleh, "The solution of the regularized long wave equation using the Fourier leap-frog method," *Zeitschrift für Naturforschung A*, vol. 65, no. 4, pp. 268–276, 2010.

[34] X. Shao, G. Xue, and C. Li, "A conservative weighted finite difference scheme for regularized long wave equation," *Applied Mathematics and Computation*, vol. 219, no. 17, pp. 9202–9209, 2013.

[35] S. Suksai and U. W. Hamphries, "Exact solutions of the regularized long-wave equation: the Hirota direct method approach to partially integrable equations," *Thai Journal of Mathematics*, vol. 5, no. 2, pp. 273–279, 2012.

[36] K. R. Raslan, K. K. Ali, and M. A. Shallal, "Solving the space-time fractional RLW and MRLW equations using modified extended tanh method with the Riccati equation," *British Journal of Mathematics & Computer Science*, vol. 21, no. 4, pp. 1–15, 2017.

[37] R. Khalil, M. Al Horani, A. Yousef, and M. Sababheh, "A new definition of fractional derivative," *Journal of Computational and Applied Mathematics*, vol. 264, pp. 65–70, 2014.

[38] T. Abdeljawad, "On conformable fractional calculus," *Journal of Computational and Applied Mathematics*, vol. 279, pp. 57–66, 2015.

[39] G. Jumarie, "Modified Riemann-Liouville derivative and fractional Taylor series of nondifferentiable functions further results," *Computers & Mathematics with Applications*, vol. 51, no. 9-10, pp. 1367–1376, 2006.